Temperature Elevation Produced by Miniature Implantable Antennas for Intracranial Pressure Monitoring

Konstantinos A. Psathas, and Konstantina S. Nikita*

School of Electrical & Computer Engineering, National Technical University of Athens,
9, Iroon Polytechniou Str., 15780 Zografos, Athens Greece
kpsathas@biosim.ntua.gr, knikita@ece.ntua.gr

Abstract

This study focuses on the assessment of the temperature distribution produced by a dual-band implantable antenna used for Intracranial Pressure Monitoring (ICP). A numerical analysis of the Specific Absorption Rate (SAR) distribution and the induced heat dissipation is presented in a spherical human head model. A temperature elevation of 0.5 - 2.7^{o}C is produced in the close proximity of the implantable antenna under compliance with the latest IEEE basic exposure limitations.

1. Introduction

Microwave energy has been extensively used in recent years as an efficient and reliable way of heating for a wide range of applications from industrial processes to cancer treatment [1]. The adoption of microwaves in everyday life resulted in an increasing public concern about potential health implications of electromagnetic fields. The guidelines for limiting exposure to radiofrequency (RF) fields [2-4], are based to a large extend on the thermal biological effects induced in human tissues. However, the safety guidelines regarding human exposure to electromagnetic fields are expressed in terms of Specific Absorption Rate (SAR) limitations rather than temperature. Evaluation of heat dissipation can complement SAR assessment in the human tissues in order to fully understand the absorption of RF energy by human tissues. Most of the studies investigating heat transfer in biological tissues use original Pennes bio-heat equation [5]. In many studies, the coupled model of Maxwell's equations and bio-heat equation has been used [6-8]. The majority of the published work about RF human exposure, though, have not studied temperature distributions produced inside human tissues, thus, the related analysis of the underlying phenomena is partially incomplete.

Moreover, most of the existing literature studying heat transfer in biological tissues have considered an RF source placed outside of the human body (in most cases the radiator is the antenna of a mobile phone). The recent interest in the use of Implantable and Ingestible Medical Devices (IIMDs) for diagnosis and treatment requires the RF source to be placed inside the human body almost in direct contact with the human tissues. Thus, the energy absorption by the neighboring tissues is expected to be high. The maximum SAR values and temperature elevation are expected to be substantially higher compared to the recorded values when the RF source is outside the human body. Studies about implantable telemetry systems [9], [10] have shown that radiation efficiency is extremely poor, indicating the difficulty of radiating out of the body, implying that a large part of the radiated power is dissipated as heat in the human tissues.

In this study, we evaluate and numerically assess the heat dissipation of a radiating implantable antenna, used for ICP [11]. The antenna operates in two bands, Medical Implant Communication Service (MedRadio, 401 – 406 MHz) and Industrial, Scientific and Medical (ISM, 2.4 – 2.48 GHz) band. The goal of this work is to provide a first insight about the heat dissipation and the temperature elevation in the human brain caused by an ICP monitoring device.

2. Models and Numerical Methods

2.1 Antenna Model

The implantable antenna model (Fig. 1) has been presented by the authors in [11] and proposed for ICP monitoring. The antenna operates in both MICS and ISM bands and features a typical planar inverted-F structure with an 11.9 mm-radius patch in serpentine configuration for increased antenna electrical length. The antenna, also, incorporates a shorting pin that connects the ground plane and the meandered patch for miniaturization purposes.

The study of heat dissipation produced by this dual band miniature antenna has been motivated by several reasons: (i) the antenna has been proposed for implantation inside human head, (b) its design has been validated by experimental measurements in [11], and (c) MICS and ISM operation can be used to highlight and evaluate the dependence of heat dissipation upon frequency.

978-1-4673-5225-3/14/$31.00 ©2014 IEEE

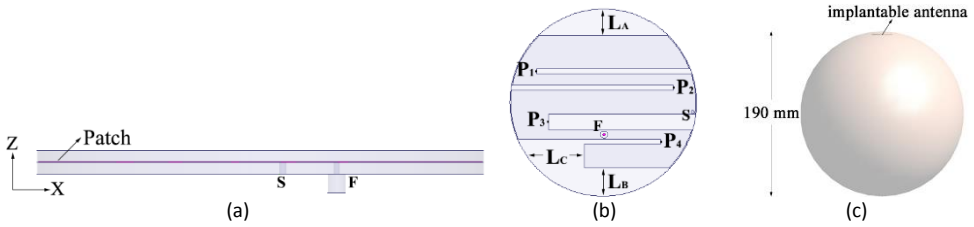

Fig. 1. (a) Side view, and (b) patch plane of the dual-band antenna used for ICP monitoring [11] and (c) homogeneous head model used for the simulations.

2.2 Tissue Model and Numerical Methods

A homogeneous spherical head model (Fig. 1(c)) is considered for electromagnetic (EM) and thermal simulations and antenna performance evaluation. Similar homogeneous or multi-layer spherical models have been extensively reported and used in the literature [12], [13]. The antenna is placed, as shown in Fig. 1, 3 mm below head's external surface (x = y = 0). The dielectric and thermal properties used in the simulations are averaged between grey matter and white matter tissue for MICS and ISM band, respectively (Table 1). The dielectric properties are considered constant in a small window around the center frequency of each band, without sacrificing the accuracy of the results [11].

Table 1. Dielectric and Thermal Properties of the tissues used in the proposed Model [14], [15]

Tissue	Dielectric Properties					Thermal Properties			
	Permittivity ε_r		*Conductivity* σ *[S/m]*		*Density* ρ *[kg/m^3]*	*Specific Heat Capacity c [J/kg/^{o}C]*	*Thermal Conductivity k [W/m/^{o}C]*	*Heat Generation Rate Q [W/kg]*	*Perfusion Rate* ω *[ml/min/kg]*
	MICS	*ISM*	*MICS*	*ISM*					
Grey Matter	57.4	49.0	0.74	1.77	1044.5	3695.8	0.547	15.53	763
White Matter	42.0	36.2	0.45	1.19	1041.0	3582.8	0.481	4.34	213
Current study	49.7	41.6	0.59	1.48	1042.7	3639.3	0.514	9.935	488

FTDT simulations are carried out using the SEMCAD X software by SPEAG [16]. A minimum spatial resolution of 72 x 100 x 158.7 μm^3 and 72 x 100 x 158.7 μm^3 and maximum spatial resolution of 35.8 x 35.5 x 37.5 mm^3 and 7.7 x 8 x 7.6 mm^3 in the x, y, and z directions is chosen for MICS and ISM band respectively. The maximum ratio of the length of two neighboring cells along an axial direction in the grid (grading ratio) is 1:2 and a percentage of local relaxation of the grading ratio to prevent over-refinement in areas with closely spaced baselines (gridding ratio relaxation) of 10% is selected. The minimum baseline resolution is set to 5 x 10^{-5} λ for MICS band and 0.0001 λ for ISM band with maximum grid cells (max step) of 0.07 λ (λ/14), with λ being the wavelength at the corresponding frequency. The max step satisfies the FDTD spatial step constraint and is conservatively chosen in an attempt to reduce dispersion errors generated by the non-uniformity of the grid. The Absorbing Boundary Conditions (ABC) are set as Uniaxial Perfectly Matched Layer (U-PML) with medium strength. Gaussian sources (pulse width of 40 periods for MICS and 90 periods for ISM – to achieve a steady state) are used for broadband simulations.

Thermal simulations are carried out based on the Pennes' Bioheat Equation (PBE) [5],

$$\rho c \frac{\partial T}{\partial t} = \nabla \cdot (k \nabla T) + \rho Q + \rho S + \rho_b c_b \rho \omega (T - T_b) \quad (1)$$

where k is the thermal conductivity, S is the SAR, ω is the perfusion rate, Q is the metabolic heat generation rate, ρ is the density of the medium, and ρ_b, c_b, and T_b are the density, specific heat capacity and temperature of the blood. The blood density and specific heat capacity are considered 1050 kg/m^3 and 3617 J/kg/^{o}C [14], [15].

The boundary condition chosen for the simulations is mixed [17] between the brain and the background, according to the equation,

$$k \frac{dT}{dn} + h(T - T_{outside}) = F_{boundary} \quad (2)$$

where $T_{outside}$ = 25^{o}C, heat transfer coefficient h = 5 W/m^2/K and heat flux = 0 ($F_{boundary}$). Heat transfer coefficient is used to emulate the thermoregulation mechanism and the sweating effect. The grid settings are the same with those used for EM simulations and the grid is optimized for thermal simulation. The total simulation time is set to 3600 s, while the thermal source's start time is set to 1800 sec.

3. Numerical Results

3.1 Antenna Performance and SAR Distribution

The simulated reflection coefficient frequency response, along with the 3D gain radiation pattern for both MICS and ISM band are shown in Fig. 3. Dual resonances are achieved in the MICS (402 MHz) and ISM (2400 MHz) bands, with wide 10 dB bandwidths of 70.1 MHz and 133.7 MHz, respectively. The antenna radiates asymmetrical far-field gain radiation patterns while implanted in the brain model, with the maximum far-field gain values calculated at -37.89 dBi and -13.81 dBi at 402 and 2400 MHz, respectively. Maximum 1g-averaged (SAR_{1g}) and 10g-averaged (SAR_{10g}) Specific Absorption Rate values are calculated for a net-input power of 1 W (Table 2). Maximum allowable input power level is subsequently computed as imposed by the latest IEEE safety standards (IEEE C95.1-1999 [2] (P_{1999}) and IEEE C95.1-2005 [3] (P_{2005})).

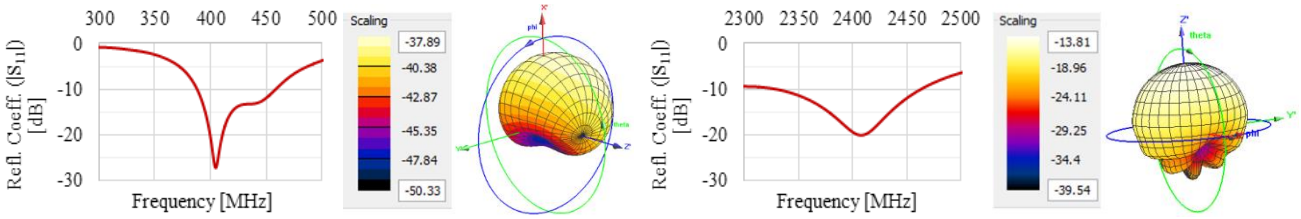

Fig. 3. Reflection coefficient ($|S_{11}|$) frequency response and 3D gain radiation pattern of the implantable antenna inside the proposed spherical brain model at (a) MICS and (b) ISM band.

Table 2. Safety Performance of the Implantable Antenna and Maximum Temperature Elevation [ΔT] inside Head

Frequency Band	SAR_{1g} [W/kg]	P_{1999} [mW]	ΔT_{P1999} [°C]	SAR_{10g} [W/kg]	P_{2005} [mW]	ΔT_{P2005} [°C]
MICS	279.00	5.73	0.4741	62.50	32.00	1.4368
ISM	225.00	7.11	0.7959	60.70	32.94	2.7049

3.2 Temperature Elevation

Thermal simulations were carried out to assess the temperature increase of the brain tissue due to the operation of the implantable antenna. Maximum temperature elevation for both P_{1999} and P_{2005} in MICS and ISM band are summarized in Table 2. Spatial temperature distributions, after 3600 sec from the start of the simulation, are shown in Fig. 4 (XZ slices, at $y = y_m$, where the maximum temperature is observed). Notable temperature elevation within the brain, as shown in Fig. 4, occurs in a very small area close to the radiating antenna. Comparing the maximum temperature elevation ΔT (Table 2), it is found that (a) the IEEE C.95.1-1999 safety standard [2] is the most strict between the two in respect to the allowable human EM field exposure in terms of SAR and consequently temperature limit, (b) the maximum temperature elevation shown in Table 2 is located in the close proximity of the implantable antenna (Fig. 4) while the temperature everywhere else in the head is limited in the range 37.3 – 37.5°C regardless of the applied safety standard. According to the literature, an increase in the temperature of the brain by 3.5°C doesn't lead to physiological damage [18].

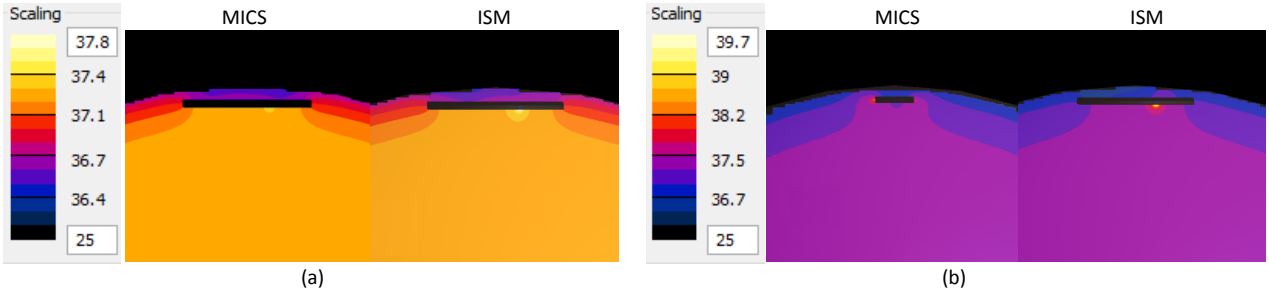

Fig. 4. Spatial temperature distribution (XZ slices) around the implantable antenna in the spherical brain model at MICS and ISM band for (a) P_{1999}, and (b) P_{2005} source input power.

4. Conclusion

In this study, we performed EM and thermal simulations to assess the temperature elevation caused in a human head model by a dual-band implantable antenna used for ICP monitoring. The results show that the maximum temperature elevation is within the range that cannot cause any physiological damage to the human brain when the antenna is fed with

input power limited by the latest IEEE safety standards. A maximum temperature elevation of 2.7°C is observed in the ISM band when the source input power is set to 32.94 mW (IEEE C.95.1-2005 [3]).

5. Acknowledgement

This work has been co-financed by the European Union (European Social Fund, ESF) and national funds, under the project THALES, ("Multilevel assessment on biological effects of radiofrequency electromagnetic waves (mBioRF))". The authors would like to thank Schmid & Partner Engineering AG (SPEAG) for providing the license for SEMCAD-X software through SEMCAD X for Science agreement.

6. References

1. P. Keangin, P. Rattanadecho, and T. Wessapan, "An analysis of heat transfer in liver tissue during microwave ablation using single and double slot antenna," *International Communications in Heat and Mass Transfer*, 2011, pp. 757-766.
2. IEEE, "IEEE Standard for Safety Levels With Respect to Human Exposure to Radio Frequency Electromagnetic Fields, 3 kHz to 300 GHz," IEEE Std C95.1-1999, 1999.
3. IEEE, "IEEE Standard for Safety Levels With Respect to Human Exposure to Radio Frequency Electromagnetic Fields, 3 kHz to 300 GHz," IEEE Std C95.1-2005, 2005.
4. ICNIRP, "Guidelines for limiting exposure to time-varying electric, magnetic, and electromagnetic fields (up to 300 GHz)," *Health Phys*, 2009, pp. 257-265.
5. H. H. Pennes, "Analysis of tissue and arterial blood temperatures in the resting human forearm," *J Appl Physiol*, 1948, pp. 93-122.
6. T. Wessapan, S. Srisawatdhisukul, and P. Rattanadecho, "Numerical Analysis of Specific Absorption Rate and Heat Transfer in the Human Body Exposed to Leakage Electromagnetic Field at 915 MHz and 2450 MHz," *Journal of Heat Transfer*, 2011, pp. 051101-051101.
7. T Wessapan, and P. Rattanadecho, "Specific Absorption Rate and Temperature Increase in Human Eye Subjected to Electromagnetic Fields at 900 MHz," *Journal of Heat Transfer*, 2012, pp. 091101-091101
8. T. Wessapan, S. Srisawatdhisukul, and P. Rattanadecho, "The effects of dielectric shield on specific absorption rate and heat transfer in the human body exposed to leakage microwave energy," *International Communications in Heat and Mass Transfer*, 2011, pp. 255-262.
9. K. Jaehoon, and Y. Rahmat-Samii, "Implanted antennas inside a human body: simulations, designs, and characterizations," *IEEE Transactions on Microwave Theory and Techniques*, 2004, pp. 1934-1943.
10. A. Kiourti, M. Christopoulou, and K.S. Nikita, "Performance of a novel miniature antenna implanted in the human head for wireless biotelemetry," *IEEE International Symposium on Antennas and Propagation (APSURSI)*, 2011.
11. A. Kiourti, K. A. Psathas, J. R. Costa, C. A. Fernandes, and K. S. Nikita, "Dual-Band Implantable Antennas for Medical Telemetry: A Fast Design Methodology and Validation for Intra-Cranial Pressure Monitoring," *Progress in Electromagnetics Research*, 2013, pp. 161-183.
12. A. Kiourti and K. S. Nikita, "Numerical assessment of the performance of a scalp-implantable antenna: effects of head anatomy and dielectric parameters," *Bioelectromagnetics*, 2013, pp. 167-79.
13. S. Koulouridis and K. S. Nikita, "Study of the coupling between human head and cellular phone helical antennas," *IEEE Transactions on Electromagnetic Compatibility*, 2004, pp. 62-70.
14. S. Gabriel, R. W. Lau, and C. Gabriel, "The dielectric properties of biological tissues: II. Measurements in the frequency range 10 Hz to 20 GHz," *Physics in Medicine and Biology*, 1996, pp. 2251-2269.
15. S. Gabriel, R.W. Lau, and C. Gabriel, "The dielectric properties of biological tissues: III. Parametric models for the dielectric spectrum of tissues," *Physics in Medicine and Biology*, 1996, pp. 2271-2293.
16. Schmid & Partner Engineering AG (SPEAG), "SEMCAD X, Ver. 14.8," 2013.
17. Schmid & Partner Engineering AG (SPEAG), "SEMCAD X Reference Manual," 2013, pp. 213-214
18. J. E. Hall, "Guyton and Hall textbook of medical physiology," 2011, Philadelphia, PA: Saunders/Elsevier.